Humanoid Robot Push-Recovery Strategy Based on CMP Criterion and Angular Momentum Regulation

Che-Hsuan Chang, Han-Pang Huang, *Member, IEEE,* Huan-Kun Hsu, and Ching-An Cheng

Abstract—We propose a push-recovery strategy to stabilize the robot under unmodelled, large external forces. The strategy integrates Center-Of-Gravity (COG) angular momentum regulator, COG state estimator, and stepping control, which online modifies the trajectories of the COG and the swing leg. Using the centroidal-moment-pivot criterion, the COG angular momentum regulator controls the dynamics of the COG as an impedance system through the feedback of COG state estimator based on Kalman filter. The stepping control, on the other hand, selects the appropriate balancing reaction in anticipation of the potential consequences of the external disturbances on the robot. In simulations and experiments, we show the proposed push-recovery strategy can effectively save the robot from falling down and walk more smoothly.

I. INTRODUCTION

In living and interacting with humans, humanoid robots face various difficulties. Especially, unexpected disturbances would unbalance a humanoid robot, causing it to fall down. Therefore, not only should a humanoid robot be able to walk stably in a perceivable environment, but it should also be equipped with strategies to recover from unexpected disturbances, such as an external push.

For stable walking, one popular way to generate balanced walking patterns is based on Zero Moment Point (ZMP) [1, 2]. In particular, simplifying the dynamics of a humanoid robot as linear inverted pendulum model (LIPM) [2, 3] further reduces the computational cost for real-time trajectory generation and control. On the other hand, inspired by biomechanical studies in human walking [4], angular momentum regulation has ever become a promising approach. Kajita et al. [5] proposed a resolved momentum control that can directly regulate the total linear/angular momentum about the Center of Gravity (COG), whose states can be estimated by using techniques such as Kalman filters [6]. Using the whole-body cooperation method developed in [7], this reference angular momentum could be transformed to reference joint velocities. Moreover, the concept of Centroidal Moment Pivot (CMP), a ground reference point with respect to which the rate of change of angular momentum is zero, introduces a model that unifies ZMP, COG and ground reaction forces. Regulating the change rate of the angular momentum about the COG, this model can be used for stable walking [4, 8], even in presence of external forces [4]. Pratt et al. [9] presented the capture point method to stabilize the robot by calculating the landing point. Similarly, Yun et al. [10] introduced a momentum-based stepping controller for the swing leg, so the

robot could recover from a large back push by taking an extra step forward.

In this paper, we propose a push-recovery strategy to stabilize the robot under unknown, large external pushes by adaptively combining different balancing reactions with respect to the estimated net pushing direction in the sagittal plane. This strategy integrates COG angular momentum regulator, COG state estimator, and stepping control, which online modifies the trajectories of the COG and the swing leg. Based on the CMP criterion, the proposed COG angular momentum regulator is designed to effectively counteract external pushes and disturbances by controlling the upper body though feeding back the ground reaction forces. In addition, with the COG state estimator, the position, velocity, and acceleration of the robot's COG used in the COG angular momentum regulator can be accessed. Finally, the stepping control is designed to adaptively select the proper balancing strategy in anticipation of the effects of external forces on the robot. The main idea is to combine the stepping control and the angular momentum regulation control, so the robot can at the same time downsize destabilizing inputs and attempt to stop safely if necessary. We implemented and integrated all these methods on a humanoid robot [11] in experiments to test the efficiency and the responses to different external forces.

II. PUSH-RECOVERY STRATEGY

When external pushes and disturbances are applied to a robot, these forces cause an uncompensated angular momentum change about the COG, making the robot unstable and the error between the desired ZMP and the actual ZMP larger. In order to increase the robustness of walking in face of external forces, we develop a push-recovery strategy to regulate the net momentum acting on the COG by online modifying the motion of the upper body and the trajectories of the COG and the swing leg. Because the maximal motor torque and the accessible joint range are limited by the mechanism design, in this paper we consider the case in which external forces are bounded and introduce a moment about the COG in the sagittal plane. In addition, we assume that the waist joint is close to the COG such that the COG can be viewed as a stationary point in the waist frame.

Under these assumptions, the inputs to the COG angular momentum regulator are measured and estimated as follows: The position, velocity and acceleration of the COG are inferred by the COG estimator using the information of IMU on robot's waist. The position of ZMP is estimated from the two six-axis force/torque sensors mounted on the ankles. The additional angular momentum caused by ground reaction forces are derived through the CMP criterion [8].

In the following, we first introduce the COG state estimator used to infer the COG's states. Then we use the information of COG and ZMP to design an impedance system to regulate the angular momentum. Finally, we combine these techniques with the stepping control so the robot can

C.-H. Chang, H.-K. Hsu, and C.-A. Cheng are with Department of Mechanical Engineering, National Taiwan University, Taipei, Taiwan (e-mail: r01522806@ntu.edu.tw, d00522029@ntu.edu.tw, and b96502138 @ntu.edu. tw).

H.-P. Huang is a professor of Department of Mechanical Engineering, National Taiwan University, Taipei, Taiwan (e-mail: hanpang@ntu. edu.tw). He is currently the director of NTU Robotics Laboratory.
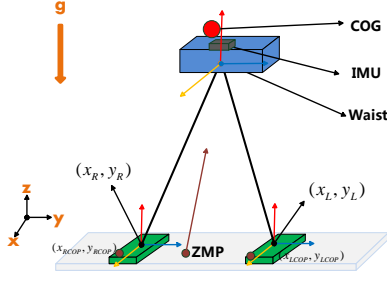
Figure 1. The system model of the COG state estimator
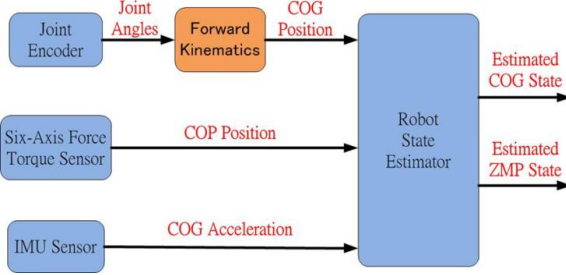
Figure 2. The block diagram of the robot state estimator

react to unknown disturbances by modifying the trajectories of the COG and the swing leg. The variables used in the following derivation are expressed in the global frame.

A. COG State Estimator

The system model of the COG state estimator is given in Fig. 1 with the governing equations [12]

$$\ddot{x}_{COG} = \frac{g}{z_0}(x_{COG} - x_{ZMP}), \tag{1}$$

where x_{COG} is the x-position of the COG, x_{ZMP} is the x-position of the ZMP, z_0 is the height of the COG, which is set constant in this paper. The model (1) is due to the identity of wrench representation. Let T be the sampling time. The discrete-time dynamics model of (1) has the state-space representation:

$$\begin{bmatrix} x_{COG,t+1} \\ \dot{x}_{COG,t+1} \\ x_{ZMP,t+1} \end{bmatrix} = \begin{bmatrix} 1 & T & 0 \\ \omega^2 T & 1 & -\omega^2 T \\ 0 & 0 & 1 \end{bmatrix} \begin{bmatrix} x_{COG,t} \\ \dot{x}_{COG,t} \\ x_{ZMP,t} \end{bmatrix} + \begin{bmatrix} 0 \\ 0 \\ T \end{bmatrix} u_t + \begin{bmatrix} \varepsilon_1 \\ \varepsilon_2 \\ \varepsilon_3 \end{bmatrix} \tag{2}$$

where $\omega^2 = g / z_o$, the lower subscript denotes the variable at time instance t, $u_t := \dot{x}_{ZMP,t}$ is the x-velocity of the ZMP, and ε is a zero-mean Gaussian noise with covariance matrix Q. We note that in (2) the velocity u_t is treated as a virtual control input.

On the other hand, we model the sensor using the following stochastic process:

$$\begin{bmatrix} \tilde{x}_{COG,t} \\ \tilde{x}_{ZMP,t} \\ \tilde{\ddot{x}}_{COG,t} \end{bmatrix} = \begin{bmatrix} 1 & 0 & 0 \\ 0 & 0 & 1 \\ \omega^2 & 0 & -\omega^2 \end{bmatrix} \begin{bmatrix} x_{COG,t} \\ \dot{x}_{COG,t} \\ x_{ZMP,t} \end{bmatrix} + \begin{bmatrix} \delta_1 \\ \delta_2 \\ \delta_3 \end{bmatrix} \tag{3}$$

where δ is a zero-mean Gaussian noise with covariance matrix R and the symbol ~ denotes the observed variables. Because the ZMP is equal to the Center Of Pressure (COP) when the robot stands on a flat horizontal plane [4], the ZMP of the robot in Fig. 1 can be calculated as
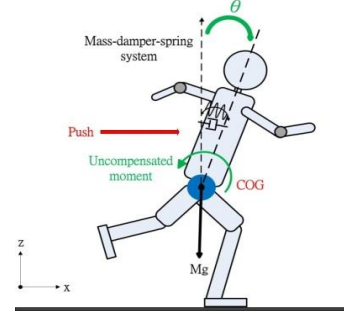
Figure 3. Model of a COG angular momentum regulator

$$x_{ZMP} = \frac{(x_L + x_{LCOP})F_{LZ} + (x_R + x_{RCOP})F_{RZ}}{F_{LZ} + F_{RZ}} \tag{4}$$

where x_L is the x-position of the left ankle, x_R is the x-position of the right ankle, x_{LCOP}, x_{RCOP} are the x-positions of the COP under two feet, and F_{LZ} and F_{RZ} are the z-force exerted by ground reaction forces on the two feet, respectively.

Thus, using Kalman filter, the forward dynamics (2), the observation (3), and (4) can be combined to estimate the states of the COG and the ZMP. The block diagram of the COG state estimator is summarized in Fig. 2.

B. CMP Criterion and COG Angular Momentum Regulator

Let x_{CMP} be the CMP's x-position. Following the CMP criterion [8], the net moment T_{COG} applied on the COG by ground reaction forces has the following equality

$$x_{CMP} = x_{COG} - \frac{F_{hor}}{F_{ver}} z_{COG} = x_{ZMP} - \frac{T_{COG}}{F_{ver}}, \tag{5}$$

or simply

$$T_{COG} = F_{ver}(x_{ZMP} - x_{COG}) + F_{hor} z_{COG}, \tag{6}$$

where F_{hor} is the ground reaction force in the horizontal direction, and F_{ver} is the ground reaction force in the normal direction. The CMP can therefore be treated as a measure of the rotational stability, which reflects the contributions of the spin angular momentum about the COG. Since T_{COG} can be calculated by (6), the rotational dynamics can be regulated as a mass-damper-spring system, as illustrated in Fig. 3, such that

$$M_d \ddot{\theta} + B_d \dot{\theta} + K_d \theta = T_{ext} - T_d \tag{7}$$

where M_d, B_d, K_d are the desired mass, damping, and stiffness which characterize the behavior of the targeted impedance, θ is the angle of COG in pitch direction, and $T_{ext} = T_{COG}$ is the moment due to external forces, and T_d is the desired angular moment which was set to zero. The parameters M_d, B_d, K_d are empirically selected by tuning the corresponding damping ratio and natural frequency so that the robot can response naturally.

C. Stepping Control

The stepping control is used to modify the trajectory of the COG and the swing leg, considering how the external disturbance would affect the robot. The first stage is to detect the push state. Because the position of the CMP is
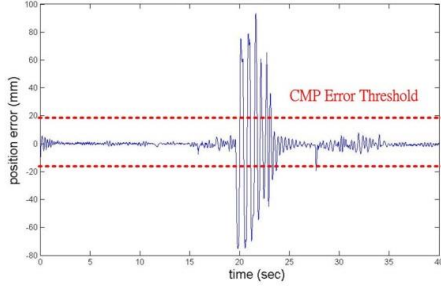
Figure 4. Threshold of COG angular momentum regulator
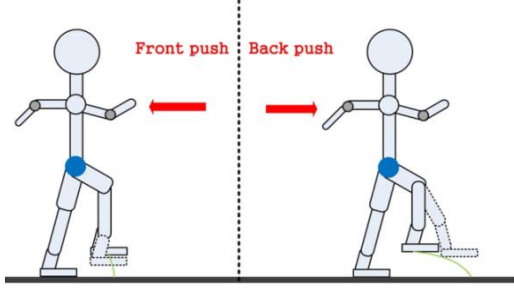
Figure 5. Push State Classification and corresponded step-ping responses

available through (5), a threshold of the error between CMP and ZMP in the sagittal plane is set to classify whether the robot is in the push state or not: if

$$\|x_{CMP} - x_{ZMP}\| \geq x_{thre} , \qquad (8)$$

the robot is considered pushed, where x_{thre} is the threshold defined by experimental results as shown in Fig. 4. x_{CMP} is calculated from the estimated COG state and the ground reaction force by (5), which is equal to x_{ZMP} when there is no net moment on the COG.

Once condition (8) is activated, the second stage further classifies the push state into front push and back push by the sign of $x_{CMP} - x_{ZMP}$ [13], and the robot is programmed to response accordingly, as shown in Fig. 5: If the push comes in front of the robot, the swing leg and the COG stop moving forward through smoothly interpolating the current trajectory with a stopping motion to place the swing leg down; once the robot recovers from the external force, the robot can resume to walk forward and continue its original task. On the contrary, if the push comes from the back, the stepping controller would calculate the new step length based on the LIPM energy method [14] and take a longer step forward [9] by the gait database, a collection of stable trajectories of the COG and the swing leg with different step lengths computed in advanced by walking pattern generator, in order to recover from the unknown external back push and maintain the balance.

To calculate the desired step length for being pushed from the back, we analyze the orbital energy E_{LIP} of the linear inverted pendulum model

$$E_{LIP} = \frac{1}{2}\dot{x}_{COG}^2 - \frac{g}{2z_0}(x_{COG} - x_{sup})^2, \qquad (9)$$

in which x_{sup} is the x-position of the support foot. E_{LIP} remains constant until the swing leg contacts the ground and the support phase changes. Therefore, assuming that the
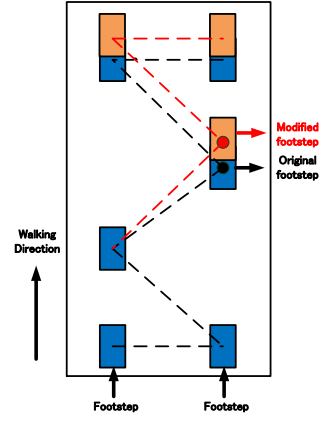
Figure 6. Modified swing leg position of back push
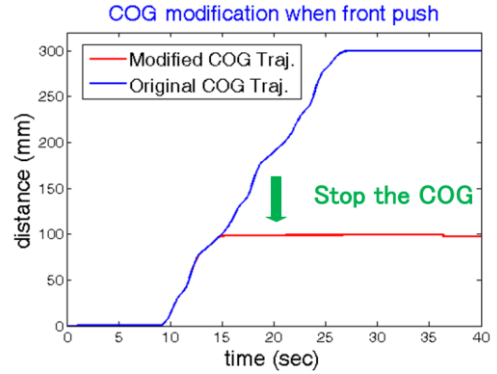
Figure 7. An exemplary modification of the COG in front push scenario
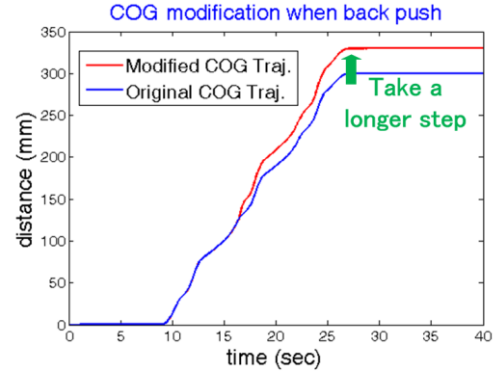
Figure 8. An exemplary modification of the COG in back push scenario

energy exchange occurs instantaneously without energy loss, the energy is conservative. In this case, the required step length can be solved based on desired orbital energy value. In this paper, we want to find the appropriate step size to stop the robot, so we set the desired E_{LIP} to zero and calculate the new location x_{new_sup} of the support foot from (9), i.e.

$$x_{new\_sup} = x_{COG} + \dot{x}_{COG}\sqrt{z_0 / g} . \qquad (10)$$

Then we modify the trajectories of the COG and the swing leg using a gait database to accomplish the task in (10). An example of the modification of the foot step and the COG trajectories are illustrated in Fig. 6–8. If the robot encounters a front push, it will stop the COG as soon as possible as shown in Fig. 7. On the contrary, if the robot encounters a back push, it will extend the trajectories of the COG and the swing leg as shown in Fig. 6 and Fig. 8.
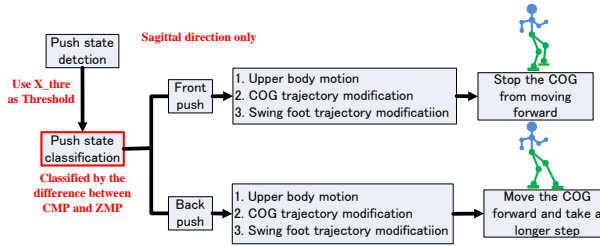
Figure 9. Push-recovery strategy control flow chart
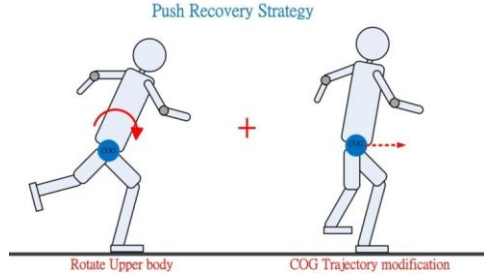
Figure 10. The push-recovery strategy scheme

D. Overall Push-Recovery Strategy

Fig. 9 and Fig. 10 show the overall push-recovery strategy control flow of the robot. According to the push state, the robot will modify the trajectories of the COG and the swing leg, either to stop the robot or to take an extra step. At the same time, the controller in (7) moves the upper body to compensate the angular momentum about the COG.

III. SIMULATIONS AND EXPERIMENTS

NINO [11], the humanoid robot developed by our laboratory, was used as the platform in the simulations and experiments (1450 mm in height, 68 kg in weight, and 200 mm in foot length). Firstly, we used MSC ADAMS to simulate the push-recovery strategy. In the simulation environment, the robot was set to perfectly track the command joint trajectories and the links were modeled as rigid bodies. As shown in Fig. 11, two simulations were implemented respectively for the front and the back pushes in sagittal plane. Secondly, we implemented the strategy experimentally on the real robot. In both cases, the sampling time was set to 5 ms. The covariance matrices Q and R in the Kalman filter are shown in Table I. R was used to model the sensor noise, which is independent of the state (the noise level in the simulation was chosen arbitrarily). Q was computed to model the error between the estimated state (recall that the current COG was approximated as a stationary point relative to the floating base) and the real state (which was known in simulations). Because such information for Q was unavailable in the experimental setting, the same covariance matrix Q was used in both the simulations and the experiments.

In the simulations, the robot walked at a constant speed for 1 step or 3 steps, in which each was 100mm long and took 6 seconds. The external push was applied on the robot from time 19.5s to 19.65s, and the magnitude was 80N. Fig 12 shows the effect of angular momentum control on the robot, which walked one step 100mm forward in the two simulations of front push. The difference is clear: the ZMP trajectory and the angular momentum about COG oscillated smaller and decayed faster to zero when the angular momentum control was applied. Fig 13 simulated the strategy for being pushed from the back, which includes COG angular momentum control and the modification of the current
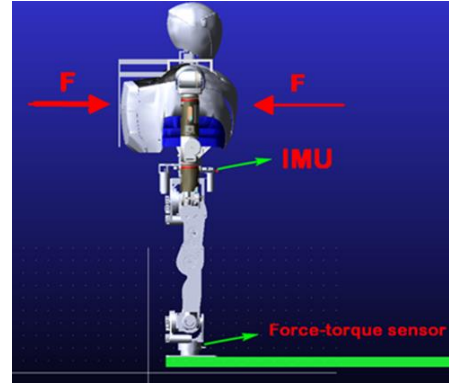
Figure 11. Settings of simulation environment in MSC ADAMS

Table I. Covariance matrices Q and R in the Kalman filter

	Simulations			Experiments		
Q	$\begin{bmatrix} 0.001 & \frac{0.001}{50} & \frac{0.001}{50} \\ \frac{0.001}{50} & 0.001 & \frac{0.001}{50} \\ \frac{0.001}{50} & \frac{0.001}{50} & 0.001 \end{bmatrix}$			$\begin{bmatrix} 0.001 & \frac{0.001}{50} & \frac{0.001}{50} \\ \frac{0.001}{50} & 0.001 & \frac{0.001}{50} \\ \frac{0.001}{50} & \frac{0.001}{50} & 0.001 \end{bmatrix}$		
R	$\begin{bmatrix} 0.01 & 0 & 0 \\ 0 & 0.001 & 0 \\ 0 & 0 & 0.001 \end{bmatrix}$			$\begin{bmatrix} 0.006 & 0 & 0 \\ 0 & 3.96 & 0 \\ 0 & 0 & 2.02 \end{bmatrix}$		

(a)

(b)

Figure 12. The simulation of external front push (a) the measured ZMP trajectory (b) the measured angular momentum about the COG

COG trajectory to step ahead. When no additional control was applied, the disturbance at about 20s caused the robot to vibrate, though the robot did not fall. By contrast, using the proposed strategy, the robot extended the step trajectory about 40 mm forward, finally stopping at about 340mm, and reduced the vibration of the robot by angular momentum

(a)

(b)
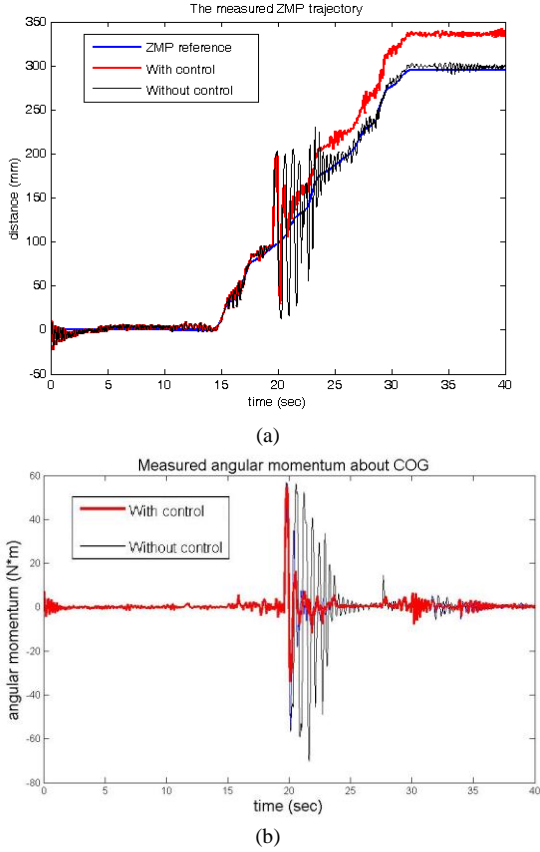
Figure 13. The simulation of external back push (a) the measured ZMP trajectory (b) the measured angular momentum about the COG

(a)

(b)

Figure 14. The experiment of external front push (a) the measured ZMP trajectory (b) the measured angular momentum about the COG

regulation, as reflected in the fluctuation of the angular momentum about COG shown in Fig. 13 (b).

The conditions of the experiments were similar to the simulations. The robot was pushed from two directions by a bag weighing 3.5kg at about 20s, resulting in an external moment below 80 Nm. The results are shown in Fig. 14 and Fig. 15. The results are similar to that in the simulations. Thanks to the push-recovery strategy, the angular momentum of COG decayed to zero quickly in 3-4 seconds and the robot continued to walk stably. Finally, the robot stopped at about 110mm position in the experiment of front push, and at about 315mm in the experiment of back push (15mm ahead of the ZMP reference due to the extended step).

IV. CONCLUSION

In this paper, a push-recovery strategy is proposed to stabilize the robot under unknown external pushes, including a COG state estimator, an angular momentum regulator based on the CMP criterion, and a trajectory modifier. Using the Kalman filter to estimate the COG's state, the angular momentum regulator performs can recover the robot to its stable posture quickly. In addition, the online COG and footstep planning strategy address two different types of pushes for the robot to maintain the stability. Therefore, when the robot is pushed, the COG angular momentum regulator is enabled, and the COG trajectory and foot step trajectory are modified correspondingly. In the simulations and experiments, the humanoid robot successfully recovered from large external forces, both in the front-push and the back-push cases. In the future, we will test this method against disturbances that affect the system in different walking phases and with different magnitudes. In addition, we will extend the CMP criterion to whole upper body, including the waist, arm, and elbow, and design an appro-
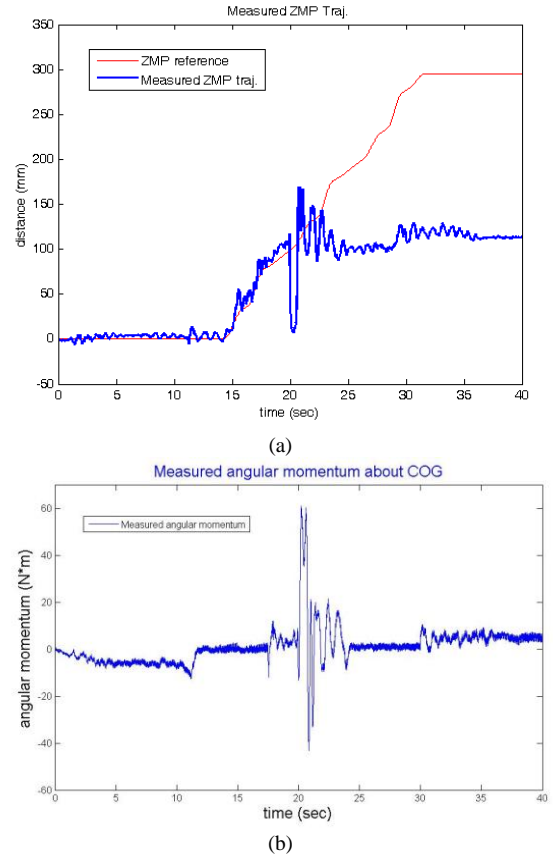
(a)

(b)
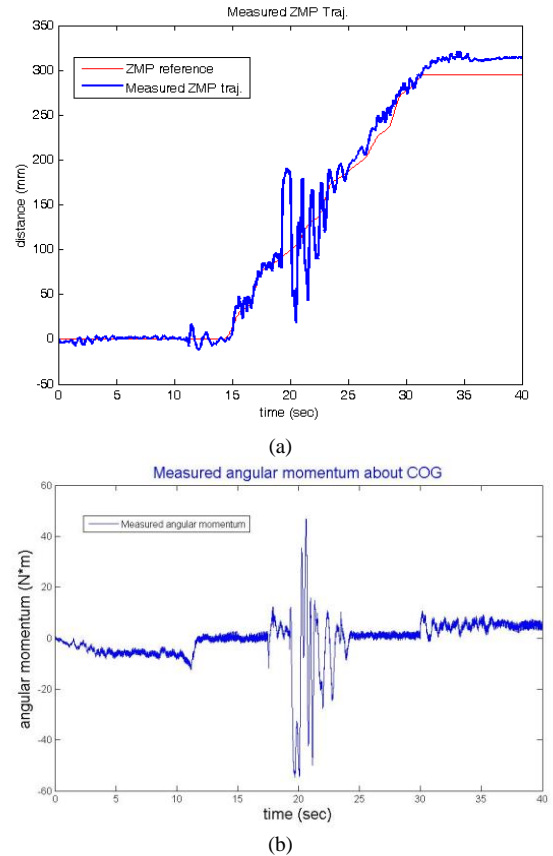
Figure 15. The experiment of external back push (a) the measured ZMP trajectory (b) the measured angular momentum about the COG

priate weighting matrix to make the humanoid robot's recovery posture and speed more similar to that of humans.

REFERENCES

[1] H.-O. Lim, Y. Yamamoto, and A. Takanishi, "Control to realize human-like walking of a biped humanoid robot," in *IEEE International Conference on Systems, Man, and Cybernetics*, 2000, pp. 3271-3276 vol.5.

[2] S. Kajita, F. Kanehiro, K. Kaneko, K. Fujiwara, K. Yokoi, and H. Hirukawa, "A realtime pattern generator for biped walking," in *IEEE International Conference on Robotics and Automation*, 2002, pp. 31-37 vol.1.

[3] K. Hirai, M. Hirose, Y. Haikawa, and T. Takenaka, "The development of Honda humanoid robot," in *IEEE International Conference on Robotics and Automation*, Leuven, Belgium, 1998, pp. 1321-1326.

[4] M. B. Popovic, A. Goswami, and H. M. Herr, "Ground reference points in legged locomotion: Definitions, biological trajectories and control implications," *I. J. Robot. Res.,* vol. 24, pp. 1013-1032, 2005.

[5] S. Kajita, F. Kanehiro, K. Kaneko, K. Fujiwara, K. Harada, K. Yokoi*, et al.*, "Resolved momentum control: humanoid motion planning based on the linear and angular momentum," in *IEEE/RSJ International Conference on Intelligent Robots and Systems*, Las Vegas, Nevada, USA, 2003, pp. 1644-1650.

[6] Xinjilefu and C. G. Atkeson, "State estimation of a walking humanoid robot," in *IEEE/RSJ International Conference on Intelligent Robots and Systems*, 2012, pp. 3693-3699.

[7] T. Sugihara and Y. Nakamura, "Whole-body cooperative balancing of humanoid robot using COG Jacobian," in *IEEE/RSJ International Conference on Intelligent Robots and Systems*, Lausanne, Switzerland, 2002, pp. 2575-2580.

[8] R. Beranek, H. Fung, and M. Ahmadi, "A walking stability controller with disturbance rejection based on CMP criterion and Ground Reaction Force feedback," in *IEEE/RSJ International Conference on Intelligent Robots and Systems*, 2011, pp. 2261-2266.

[9] J. Pratt, J. Carff, S. Drakunov, and A. Goswami, "Capture Point: A Step toward Humanoid Push Recovery," in *IEEE-RAS International Conference on Humanoid Robots*, Genova, Italy, 2006, pp. 200-207.

[10] S.-k. Yun and A. Goswami, "Momentum-based reactive stepping controller on level and non-level ground for humanoid robot push recovery," in *IEEE/RSJ International Conference on Intelligent Robots and Systems*, 2011, pp. 3943-3950.

[11] H.-Y. Lee, H.-P. Huang, and H.-K. Hsu, "Lifting motion planning for humanoid robots," in *IEEE International Conference on Automation Science and Engineering*, Taipei,Taiwan, 2014, pp. 1174-1179.

[12] T. Sugihara, Y. Nakamura, and H. Inoue, "Real-time humanoid motion generation through ZMP manipulation based on inverted pendulum control," in *IEEE International Conference on Robotics and Automation*, 2002, pp. 1404-1409.

[13] A. Yasin, Q. Huang, Q. Xu, and W. Zhang, "Biped robot push detection and recovery," in *International Conference on Information and Automation*, 2012, pp. 993-998.

[14] J. E. Pratt and S. V. Drakunov, "Derivation and Application of a Conserved Orbital Energy for the Inverted Pendulum Bipedal Walking Model," in *IEEE International Conference on Robotics and Automation*, 2007, pp. 4653-4660.